Climate Dynamics (2019) 52:6195–6212
https://doi.org/10.1007/s00382-018-4504-9

Effect of excessive equatorial Pacific cold tongue bias on the El Niño-Northwest Pacific summer monsoon relationship in CMIP5 multi-model ensemble

Gen Li[1] · Yuntao Jian[2] · Song Yang[2,3] · Yan Du[4] · Ziqian Wang[2,3] · Zhenning Li[2] · Wei Zhuang[5] · Wenping Jiang[1,6] · Gang Huang[6]

Received: 14 May 2018 / Accepted: 15 October 2018 / Published online: 19 November 2018

Abstract
El Niño induces an anomalous lower-tropospheric anticyclone over the tropical Northwest Pacific (NWP), accompanied by suppressed local convection and rainfall. The tropical NWP anomalies persist until the following summer, with major effects on the Asian summer monsoons. Based on the phase 5 of the Coupled Model Intercomparison Project (CMIP5) multi-model ensemble, this study finds that climate models commonly underestimate this El Niño-NWP teleconnection with too weak tropical NWP anticyclone and rainfall anomalies in post-El Niño summers, potentially limiting the models' skill in seasonal prediction of the Asian summer monsoons. The analyses show that such underestimated NWP anomalies in post-El Niño summers in CMIP5 models can be traced back to the well-known excessive equatorial Pacific cold tongue error in the mean. Models with an excessive westward extension of Pacific cold tongue tend to displace westward the simulated pattern of El Niño-related warm SST anomalies along the equator. The warm SST biases over the western Pacific in CMIP5 models would enhance the local atmospheric convection/rainfall and induce low-level cyclonic circulation anomalies over the tropical NWP with a Gill-type Rossby wave response, resulting in the commonly underestimated NWP anticyclone and rainfall anomalies during post-El Niño summers. The present results, along with our previous finding that the equatorial cold tongue bias would distort the projections of tropical Pacific warming pattern under increased greenhouse gas scenario, imply that reducing equatorial cold tongue bias in models can substantially improve climate simulation and prediction/projection for the tropical Pacific and Asian monsoons.

Keywords Equatorial Pacific cold tongue · Model error · El Niño · Tropical Northwest Pacific anticyclone · Asian summer monsoons · Matsuno-Gill dynamics

1 Introduction

El Niño events are characterized by anomalous warming of sea surface temperature (SST) in the central and eastern equatorial Pacific on interannual timescale, exerting profound impacts on weather and climate around the globe (Zhang et al. 1996; Trenberth et al. 1998; Huang and Wu 1989; Webster and Yang 1992; Klein et al. 1999; Wang et al. 1999, 2006; Alexander et al. 2002; Wu et al. 2003; Du et al. 2011). For instance, El Niño remotely influences the

✉ Gen Li
ligen@hhu.edu.cn

[1] College of Oceanography, Hohai University, Nanjing, China

[2] Institute of Earth Climate and Environment System, School of Atmospheric Sciences, Sun Yat-sen University, Guangzhou, China

[3] Guangdong Province Key Laboratory for Climate Change and Natural Disaster Studies, Sun Yat-sen University, Guangzhou, China

[4] State Key Laboratory of Tropical Oceanography, South China Sea Institute of Oceanology, Chinese Academy of Sciences, Guangzhou, China

[5] State Key Laboratory of Marine Environmental Science and College of Ocean and Earth Sciences, Xiamen University, Xiamen, China

[6] State Key Laboratory of Numerical Modeling for Atmospheric Sciences and Geophysical Fluid Dynamics, Institute of Atmospheric Physics, Chinese Academy of Sciences, Beijing, China

interannual variability of monsoon circulation and rainfall over the tropical Northwest Pacific (NWP) through atmospheric teleconnections (Wang et al. 2000) and/or by inducing the tropical Indian Ocean (IO) SST response (Yang et al. 2007; Xie et al. 2009; Kosaka et al. 2013).

As a result of the remote forcing from the equatorial Pacific SST warming, an anomalous lower-tropospheric anticyclone develops rapidly over the tropical NWP during the El Niño mature phase (usually boreal winter; Wang et al. 2000). This anomalous El Niño-induced anticyclone over the tropical NWP can persist from winter to the following summer (Yang et al. 2007; Xie et al. 2009). Accompanied by suppressed local convection and rainfall, the anomalous summer NWP anticyclone is part of the Pacific-Japan pattern (Nitta 1986, 1987) [also known as the East Asia-Pacific pattern (Huang and Sun 1992)] with important climatic effects on the East Asian summer monsoon to the north (Huang and Wu 1989; Chang et al. 2000) and the South Asian summer monsoon to the west (Mishra et al. 2012; Li et al. 2017). For example, the anomalous anticyclone in a post-El Niño summer would prevent the seasonal northward migration of the East Asian Meiyu-Baiu rain band and bring anomalously wet and cool conditions to the Yangtze River valley, Korea, and Japan (e.g., the great Yangtze River flood during the summer of 1998) via the Pacific-Japan pattern (Chowdary et al. 2011), as well as reduce land rainfall over the eastern Indo-Gangetic Plain through weakening the South Asian monsoon winds (Chowdary et al. 2013). The anomalous tropical NWP anticyclone during El Niño decaying summers is a key system that bridges the equatorial Pacific El Niño events and Asian summer monsoon circulation/rainfall variabilities. Therefore, the correlation between the anomalous summer anticyclone over the tropical NWP and the preceding winter El Niño is a potential source of seasonal predictability of the Asian summer monsoons that could benefit the socioeconomic livelihood of billions of people.

During the past two decades, studies have been conducted to understand the physical mechanisms for the El Niño-NWP anticyclone teleconnection. For example, Wang et al. (2000) suggested that the development and persistence of the anomalous El Niño-excited anticyclone result primarily from the coupling with local SST cooling via a Rossby-wave response. A nonlinear interaction mechanism between atmospheric responses to interannual El Niño SST anomalies of the tropical Pacific and the background annual cycle is also suggested to be responsible for the rapid growth of anomalous anticyclone (Stuecker et al. 2013, 2015). Another hypothesis suggests that El Niño-induced IO basin (IOB) warming can persist through the following summer when El Niño-related SST anomalies have largely dissipated over the equatorial Pacific (Yang et al. 2007; Xie et al. 2009; Yoo et al. 2006). It can contribute to the suppressed summer convection/rainfall and anticyclonic circulation anomalies over the tropical NWP through exciting a warm Kelvin wave penetrating into the equatorial western Pacific (Xie et al. 2009). On the other hand, the anomalous easterly winds on the south flank of the anticyclone warm the North IO SST by weakening the monsoon westerlies and reducing surface evaporation (Du et al. 2009; Kosaka et al. 2013). The air-sea coupling between the anticyclone and North IO warming under the summer monsoon westerlies constitutes a positive feedback (Xie et al. 2009; Kosaka et al. 2013; Li et al. 2016a). This is known as the Indo-western Pacific Ocean capacitor (IPOC) effect (Xie et al. 2016), illustrating the importance of interannual IOB SST warming for anomalous tropical NWP anticyclone during the summers following El Niño.

Figure 1 compares the composited anomalies of precipitation, sea level pressure (SLP), and 850-hPa winds in post-El Niño summers between observations and the multi-model ensemble (MME) mean simulations of 20 coupled general circulation models (CGCMs; see Table 1). The CGCM outputs are derived from the historical simulations in phase 5 of the Coupled Model Intercomparison Project (CMIP5; Taylor et al. 2012). Observations show that the anomalous lower-tropospheric anticyclone accompanied by negative convection/rainfall anomalies appears over the tropical NWP during El Niño decaying summers. In contrast, the tropical NWP anticyclone and negative rainfall anomalies in post-El Niño summers are much weaker in the CMIP5 MME mean simulations compared to observations, potentially limiting the models' skill in seasonal prediction of the Asian summer monsoons (Nitta 1987; Huang and Wu 1989; Chang et al. 2000; Chowdary et al. 2011; Mishra et al. 2012; Li et al. 2017). It is unclear whether such underestimated circulation and rainfall anomalies over the tropical NWP in CMIP5 CGCMs are ascribed to the simulated biases in El Niño or IOB amplitudes.

Previous studies suggested that the underestimated El Niño-NWP summer monsoon relationship in CGCMs might be originated from the biases in tropical IO SST anomalies (Hu et al. 2014) or SST anomaly gradients between the tropical IO and equatorial western Pacific (Jiang et al. 2017) during El Niño decaying summers. However, the present study suggests that the errors in tropical IO SST anomalies are not important for the simulated biases of anomalous NWP summer anticyclone, and emphasizes the key role of an excessive westward extension of El Niño-related warm SST anomalies in the underestimated relationship between El Niño and anomalous tropical NWP summer anticyclone in CGCMs. This is reminiscent of the excessive westward extension of equatorial Pacific cold tongue that is a common bias for the tropical climate simulation in the mean state (Li et al. 2015) and has persisted in several generations of climate models over two decades (Mechoso et al. 1995; Yu and Mechoso

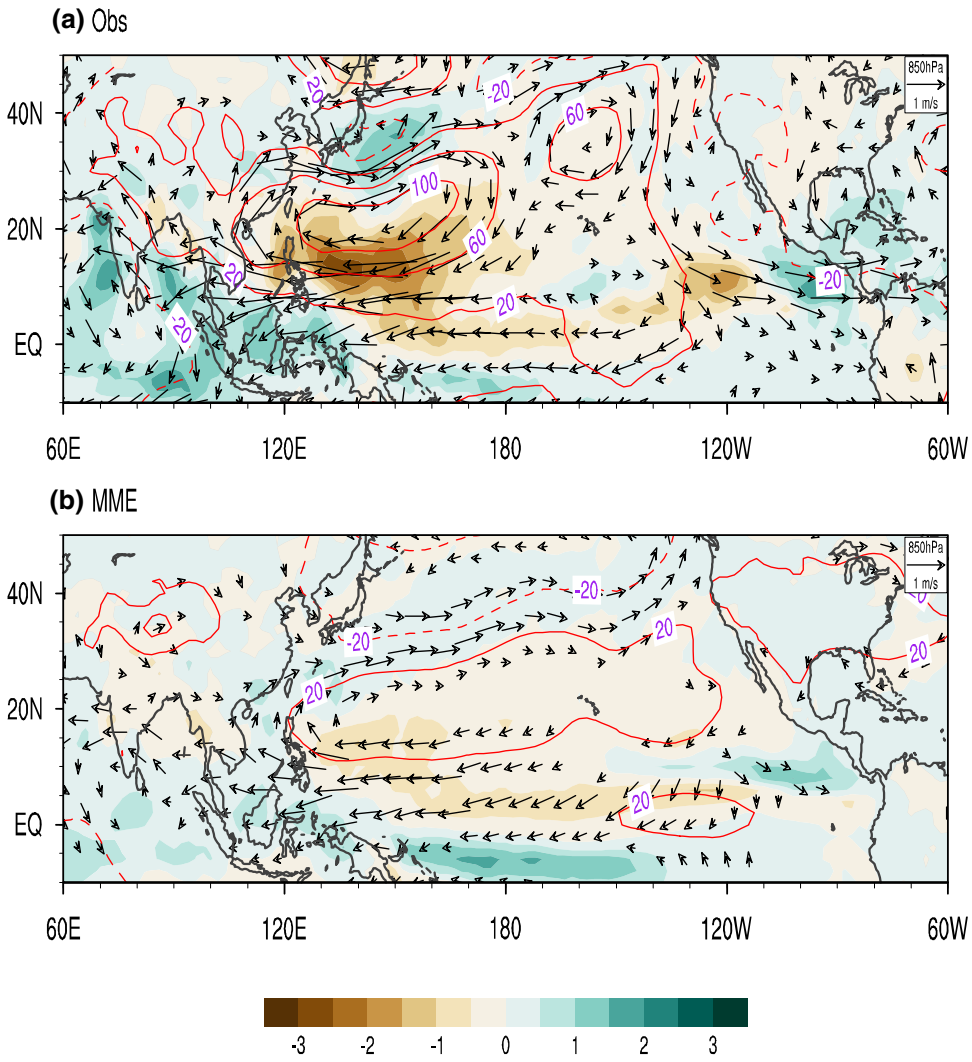

Fig. 1 Composited anomalies of precipitation (color shaded, mm/day), SLP (contours, Pa), and 850-hPa winds (vectors, m/s) for El Niño decaying summers (June–August) between **a** observations and **b** the multi-model ensemble (MME) mean simulations of 20 coupled general circulation models (CGCMs). The wind speed smaller than 0.2 m/s has been masked out

1999; Latif et al. 2001; Lin 2007; de Szoeke and Xie 2008; Li and Xie 2012, 2014; Zheng et al. 2012; Li et al. 2016b).

This study examines the nature and source of the biases in tropical NWP monsoon circulation and rainfall anomalies during El Niño decaying summers in 20 CMIP5 CGCMs. We show that CMIP5 CGCMs commonly underestimate the anomalous anticyclone over the tropical NWP in post-El Niño summers. Our analysis reveals that such biases of the El Niño-NWP summer monsoon teleconnection in CGCMs can be traced back to the equatorial Pacific cold tongue bias in the mean. Models with an excessive extension of equatorial Pacific cold tongue tend to displace westward the simulated pattern of El Niño-related warm SST anomalies. The resultant warm SST biases over the western Pacific would enhance the local atmospheric convection/rainfall and induce low-level cyclonic circulation anomalies over the tropical NWP with a Gill-type Rossby wave response, artificially weakening the NWP anomalous anticyclone. Our results highlight the importance of a realistic equatorial Pacific cold tongue simulation in the mean state for reducing the errors of El Niño SST anomaly pattern and its NWP climate teleconnections in CGCMs.

The rest of this paper is organized as follows. In Sect. 2, we describe the models, datasets, and methods used in this study. Section 3 provides a brief description of the biases in tropical NWP monsoon circulation and rainfall anomalies during El Niño decaying summers in CMIP5 CGCMs. Section 4 investigates the possible sources of the commonly underestimated anomalous anticyclone over the tropical NWP in post-El Niño summers and traces the errors back to the excessive equatorial Pacific cold tongue bias in the mean in CGCMs. Section 5 is a summary with discussions.

Table 1 A list of 20 CMIP5 models used in this study

Model name	Model group (or center)
ACCESS1-0	CSIRO-BOM
bcc-csm1-1-m	BCC
CanCM4	CCCMA
CanESM2	CCCMA
CCSM4	NCAR
CESM1-FASTCHEM	NCAR
CESM1-WACCM	NSF-DOE-NCAR
CMCC-CMS	CMCC
FIO-ESM	SOA
GFDL-CM3	NOAA GFDL
HadCM3	MOHC
HadGEM2-AO	MOHC
inmcm4	INM
IPSL-CM5A-LR	IPSL
IPSL-CM5A-MR	IPSL
MIROC5	MIROC
MPI-ESM-LR	MPI-M
MPI-ESM-MR	MPI-M
MRI-CGCM3	MRI
NorESM1-ME	NCC

2 Models, datasets, and methods

2.1 Models and datasets

We examine the monthly mean outputs of the historical runs from 20 CMIP5 CGCMs (Taylor et al. 2012). Table 1 shows the model names and modeling groups (or centers). Further information on individual models is available online at http://cmip-pcmdi.llnl.gov/cmip5/availability.html. Precipitation, sea surface temperature (SST), sea level pressure (SLP), zonal and meridional winds at 850 hPa and 200 hPa, and tropospheric temperature from 850 to 200 hPa are used. Here, we only use one ensemble member ("r1i1p1") run for each model. The MME mean in this study is defined as the composite average of all El Niño events identified in 20 CMIP5 CGCMs, unless otherwise specified.

For comparison, we examine the observed and reanalyzed (assimilated) datasets (for simplicity referred to as observations). Specifically, the precipitation is obtained from the Climate Prediction Center (CPC) Merged Analysis of Precipitation (CMAP; Xie and Arkin 1997). The SST is gained from the National Oceanic and Atmospheric Administration (NOAA) Extended Reconstructed Sea Surface Temperature (ERSST; Smith et al. 2008). The SLP, zonal and meridional winds, and tropospheric temperature from the National Centers for Environmental Prediction-National Center for Atmospheric Research (NCEP-NCAR) reanalysis project (Kalnay et al. 1996) are used. We also examine the European Centre for Medium-Range Weather Forecasts (ECMWF) reanalysis data for SLP, and zonal and meridional winds (ERA-Interim; Dee et al. 2011). The results from the ERA-Interim reanalysis are almost identical to the NCEP-NCAR reanalysis, and are therefore not shown in this study. All model outputs and observational datasets are interpolated to a uniform $2° \times 2°$ horizontal grid. In this study, we examine the 1979–2005 period for both model outputs and observational datasets owing to the data availability and reliability, unless otherwise specified. We also extend the present analysis period to 1948–2005 by using the NCEP-NCAR reanalysis data. The results (not shown) are very similar to the 1979–2005 period, documenting the robustness of the present results.

2.2 Definitions of the El Niño events and anomalous NWP anticyclone indices

We identify El Niño events based on the Ocean Niño Index (ONI), which is 3-month running mean of SST anomalies in the Niño3.4 region (170°W–120°W, 5°N–5°S). The ONI exceeding 0.5 °C for at least five consecutive months and reaching a mature phase in boreal winters defines an El Niño event. Further information about ONI is available online at http://origin.cpc.ncep.noaa.gov/products/analysis_monitoring/ensostuff/ONI_v5.php from the CPC in NOAA. Here we examine the El Niño events based on the 1979–2005 period in both observations and models, unless otherwise specified.

To quantitatively represent the atmospheric circulation and rainfall variabilities associated with the El Niño-induced anomalous anticyclone over the tropical NWP, we introduce three indices for boreal summers. The NWP monsoon circulation index associated with anomalous summer anticyclone (hereafter UI) is defined as the difference of the averaged 850-hPa zonal wind anomalies between the two regions (100°E–130°E, 5°N–15°N and 110°E–140°E, 20°N–30°N), following the work of Wang et al. (2001). The NWP anticyclone is in essence a Gill-type Rossby wave circulation response to the convective heating caused by the NWP precipitation anomalies (Fig. 1a; also see Wang et al. 2000; Xie et al. 2009; Lu and Lu 2015; Liu et al. 2018). The NWP precipitation index (hereafter PRI) is defined as the precipitation anomalies averaged over the region (110°E–160°E, 10°N–20°N), following the work of Lu and Lu (2015). Actually, the correlation coefficient between the observed UI and PRI reaches up to 0.83, exceeding the 0.001 significance level according to the Student's *t* test. Both the UI and PRI reflect identical summer variability associated with anomalous tropical NWP anticyclone, but from the viewpoint of atmospheric circulation and rainfall, respectively. In addition, the anomalous NWP anticyclone is accompanied with a rise of local SLP, as shown in Fig. 1a.

Therefore, we also define a SLP index (hereafter SLPI) using the difference of the SLP anomalies between the averages over the two regions (120°E–170°E, 15°N–25°N and 120°E–170°E, 5°S–5°N). The correlation coefficient between the SLPI and UI in observations is as high as −0.81, exceeding the 0.001 significance level according to the Student's *t* test.

2.3 Sensitivity experiment

We perform a sensitivity experiment using the Community Atmosphere Model version 4 (CAM4; Gent et al. 2011) developed by the NCAR. First, we prepare three types of SST fields: SST0, SST1, and SST2. SST0 is the global climatological SST with seasonal cycle during 1979–2008 derived from observations (Hurrell et al. 2008). SST1 is the composited monthly SST anomalies over the tropics (20°S–20°N) for the El Niño decaying years during the period of 1979–2005 from the ERSST. SST1 outside the tropics is set to zero. SST2 is the bias pattern of El Niño SST anomalies over the tropical Pacific (120°E–80°W, 20°S–20°N) related to the equatorial Pacific cold tongue bias. SST2 is shown in the black box of Fig. 9d, and set to zero outside the tropical Pacific. Two Atmospheric Model Intercomparison Project (AMIP)-type experiments are performed: Exp_CNTL, a control run forced by (SST0 + SST1), and Exp_SE, a sensitivity run forced by (SST0 + SST1 + SST2). We run the experiments for 30 years and the average of the last 20 years is analyzed. The differences between the Exp_SE and Exp_CNTL represent the atmospheric responses to the bias pattern of El Niño SST anomalies related to the equatorial Pacific cold tongue bias.

3 Model biases in the tropical NWP monsoon circulation/rainfall anomalies

Figure 2 examines the relationships between the tropical NWP pressure (anticyclonic) and rainfall anomalies during El Niño decaying summers among observations and 20

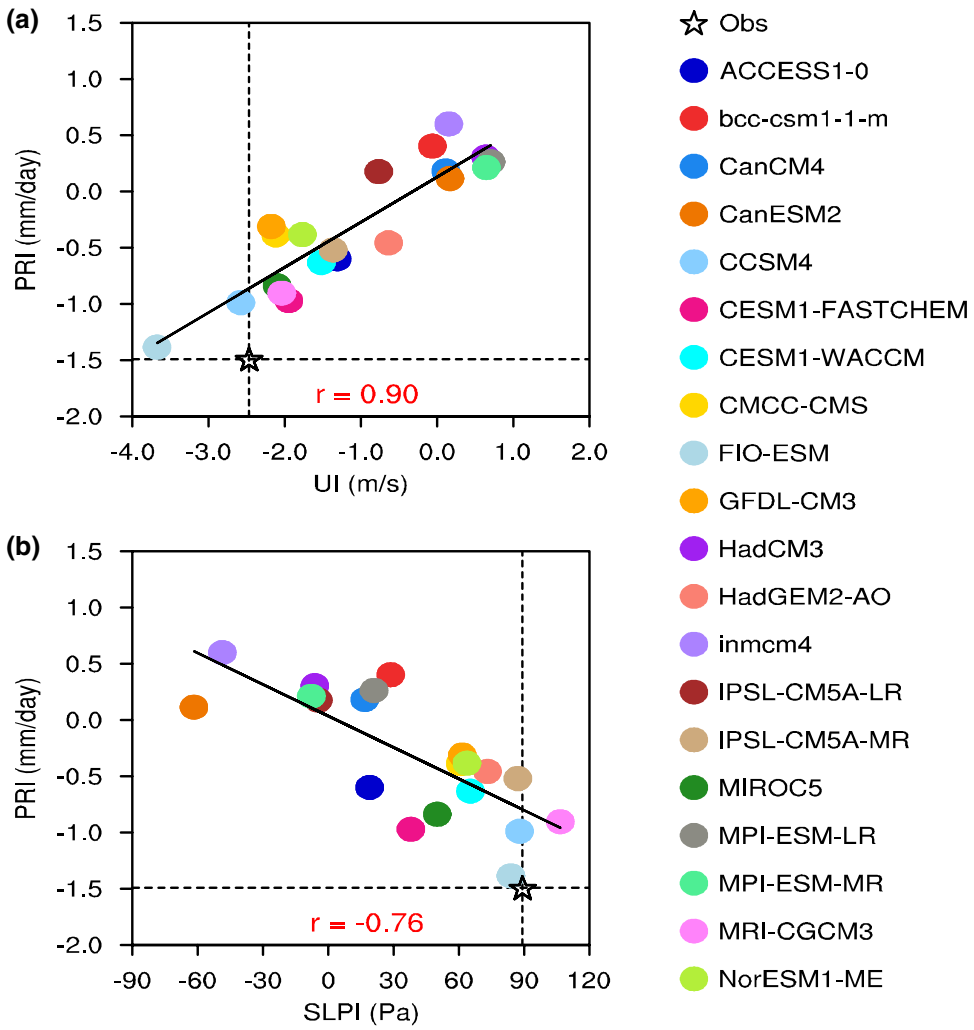

Fig. 2 Relationships of the PRI with **a** UI and **b** SLPI during El Niño decaying summers among observations and 20 CMIP5 CGCMs. The inter-model correlation (r) is shown at the bottom in each panel

CMIP5 CGCMs. The CMIP5 CGCMs commonly simulate too weak tropical NWP pressure (anticyclonic) and negative rainfall anomalies during post-El Niño summers. The inter-model variations in the NWP summer SLP (anticyclonic) and rainfall anomalies are considerable. Some models (e.g. CanESM2, HadCM3, inmcm4, and MPI-ESM-MR) even have low-level cyclonic circulation and positive rainfall anomalies over the tropical NWP during El Niño decaying summers. Models with weaker (stronger) negative rainfall anomalies tend to produce physically consistent weaker (stronger) low-level anticyclonic circulation and positive SLP anomalies, with the inter-model correlations of 0.90 and −0.76, respectively. Statistically, both the inter-model correlation coefficients exceed the 0.001 significance level according to the Student's *t* test. This feature is suggestive of a Rossby wave circulation response to the convective heating associated with NWP rainfall anomalies, in terms of the Matsuno (1966) and Gill (1980) dynamics.

4 Origin of the anomalous tropical NWP anticyclone/rainfall biases

4.1 The El Niño and IOB amplitudes

As we have known, the summer pressure (anticyclonic) and rainfall anomalies over the tropical NWP are closely associated with the IOB SST warming (Yang et al. 2007; Xie et al. 2009) that is induced by the preceding winter El Niño and sustained by mutual ocean–atmosphere interactions between the tropical IO and NWP (Kosaka et al. 2013; Xie et al. 2016). Here we examine whether the underestimated tropical NWP circulation/rainfall anomalies in CMIP5 CGCMs are originated from the simulated biases in El Niño or IOB amplitudes. Figure 3a, b compare the composited monthly mean Niño3.4 and IOB SST anomalies from January of the El Niño development year to December of the following year between observations and the MME simulations, respectively. Compared to observations, CMIP5 CGCMs satisfactorily reproduce the El Niño phase locking with the tendency of Niño3.4 SST anomalies to peak during boreal winters and decay rapidly during the following springs as well as the El Niño SST anomaly amplitudes. The inter-model relationship between the simulated tropical NWP anticyclonic anomalies and El Niño amplitudes is not statistically significant (r = −0.14; Fig. 4a), suggesting that the commonly underestimated NWP circulation/rainfall anomalies during decaying El Niño summers in CMIP5 CGCMs are not associated with the simulated biases in El Niño amplitudes.

CMIP5 CGCMs also reproduce the evolution of interannual IOB SST anomalies very well, including a peculiar double-peak IOB SST warming with the second peak persisting through the decaying El Niño summers. The simulated IOB

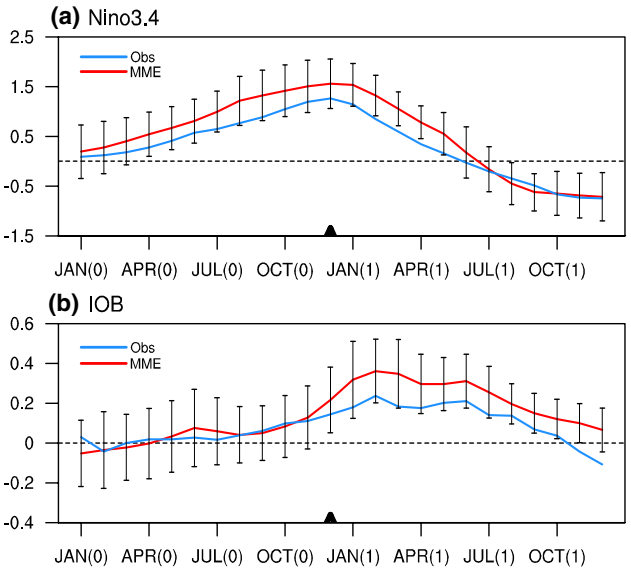

Fig. 3 Comparisons of composited monthly mean SST (°C) anomalies for the **a** Niño3.4 region (170°W–120°W, 5°N–5°S) and **b** Indian Ocean basin (IOB; 20°S–20°N, 40°E–110°E) from January of the El Niño development year to December of the following year between observations and the MME simulations. The black triangle at the bottom in each panel denotes December of the El Niño development year. Error bars for the MME simulations indicate the standard deviation spread among 20 CMIP5 CGCMs

SST warming amplitudes in CMIP5 CGCMs are comparable to the observed one (Fig. 3b). While CGCMs with a stronger El Niño amplitude tend to feature a larger interannual IOB SST warming amplitude with the inter-model correlation of 0.59 exceeding the 0.01 significance level according to the Student's *t* test (Fig. 4c), the inter-model relationship between the simulated tropical NWP anticyclonic anomalies and interannual IOB warming amplitudes is not statistically significant (r = −0.26; Fig. 4b). All this suggests that the common underestimation of tropical NWP circulation and rainfall anomalies during decaying El Niño summers in CMIP5 CGCMs does not originate from the simulated biases in El Niño or IOB amplitudes.

4.2 The mean cold tongue bias

To explore the source of the underestimated El Niño-NWP summer monsoon relationship in CMIP5 CGCMs, we choose four models (CanESM2, HadCM3, MPI-ESM-LR, and MPI-ESM-MR) as the strong tropical NWP anticyclone bias ($NWPAC^-$) models, and four models (CCSM4, FIO-ESM, GFDL-CM3, and MIROC5) as the weak and non-tropical NWP anticyclone bias ($NWPAC^+$) models based on the UI as shown in Fig. 2a. Indeed, while $NWPAC^+$ models well capture the tropical NWP anticyclonic and rainfall anomalies, $NWPAC^-$ models have too weak anticyclonic

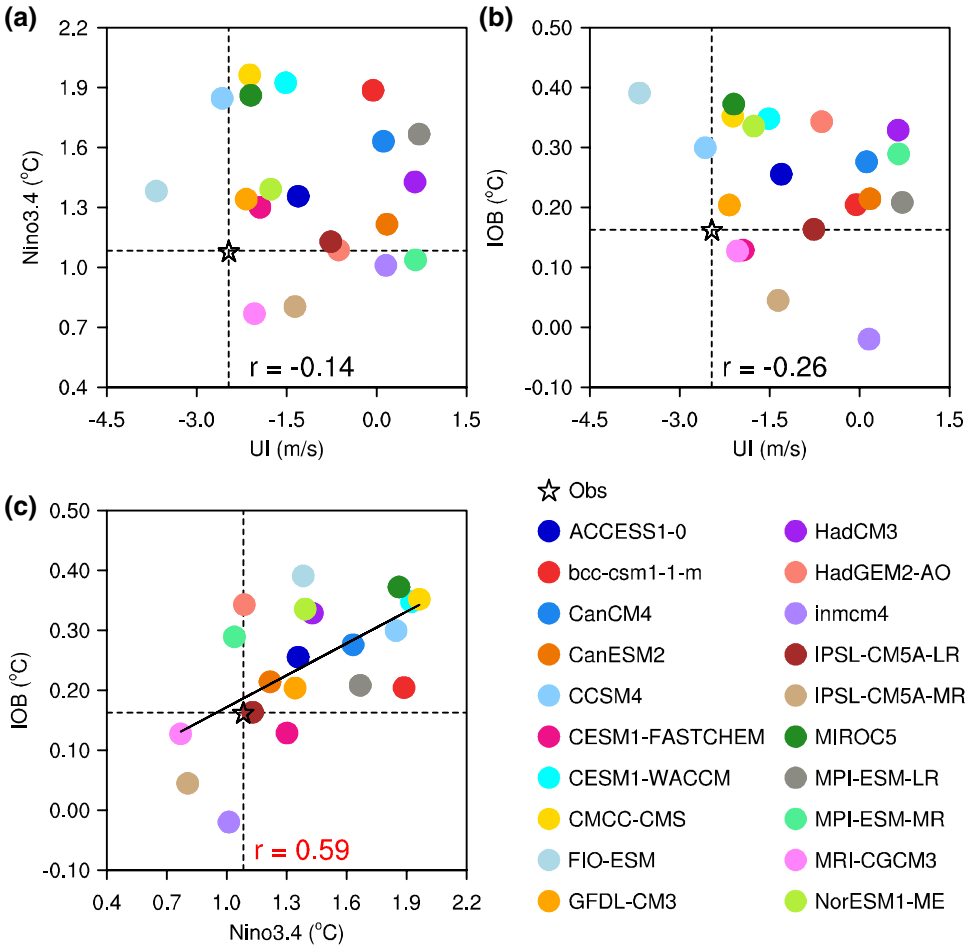

Fig. 4 Scatterplots of the UI versus **a** Niño3.4 SST anomalies during El Niño mature winters (from December of the El Niño development year to February of the following year) and **b** IOB SST anomalies during El Niño decaying summers and **c** the Niño3.4 SST anomalies during El Niño mature winters versus IOB SST anomalies during El Niño decaying summers among observations and 20 CMIP5 CGCMs. The inter-model correlation (r) is shown at the bottom in each panel

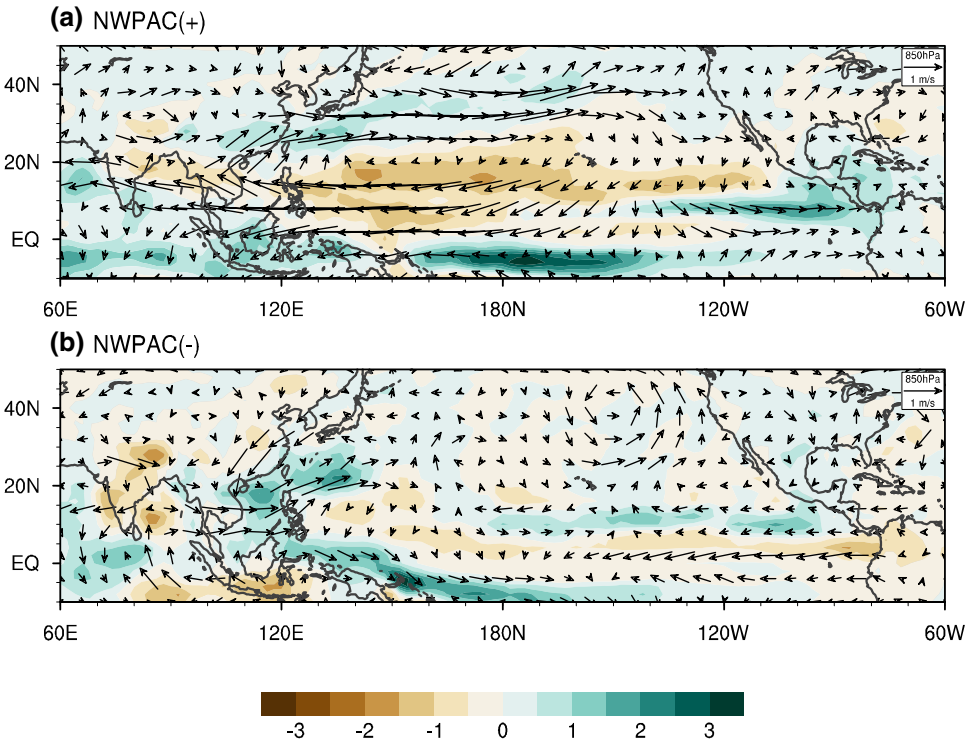

Fig. 5 Composited anomalies of precipitation (color shaded, mm/day) and 850-hPa winds (vectors, m/s) during El Niño decaying summers for **a** NWPAC^{+} models and **b** NWPAC^{-} models

and rainfall anomalies in post-El Niño summers (Fig. 5). All the analysis results based on the SLPI and PRI are also very similar, and thus we only give the results based on the UI in this study, unless otherwise specified.

Figure 6a–c show the composited SST anomalies over the tropical Pacific and IO during El Niño mature winters for observations, NWPAC$^+$ models, and NWPAC$^-$ models, respectively. Both the NWPAC$^+$ models and NWPAC$^-$ models represent interannual SST warming over the central and eastern equatorial Pacific, with comparable magnitude to observations. We note that, however, the equatorial Pacific SST warming in NWPAC$^-$ models penetrates too far westward than those in observations and NWPAC$^+$ models. Figure 6d shows the composited El Niño SST anomaly difference between NWPAC$^-$ and NWPAC$^+$ models. Statistically significant warm SST anomalies appear over the equatorial western Pacific for simulated El Niño events between NWPAC$^-$ models and NWPAC$^+$ models, consistent with the excessive westward extension of equatorial Pacific SST warming in NWPAC$^-$ models. Similar warm SST anomaly biases between NWPAC$^-$ models and observations also exist over the equatorial western Pacific (figure not shown). In particular, the multi-model statistics (Fig. 7) indicates that models with warm biases in

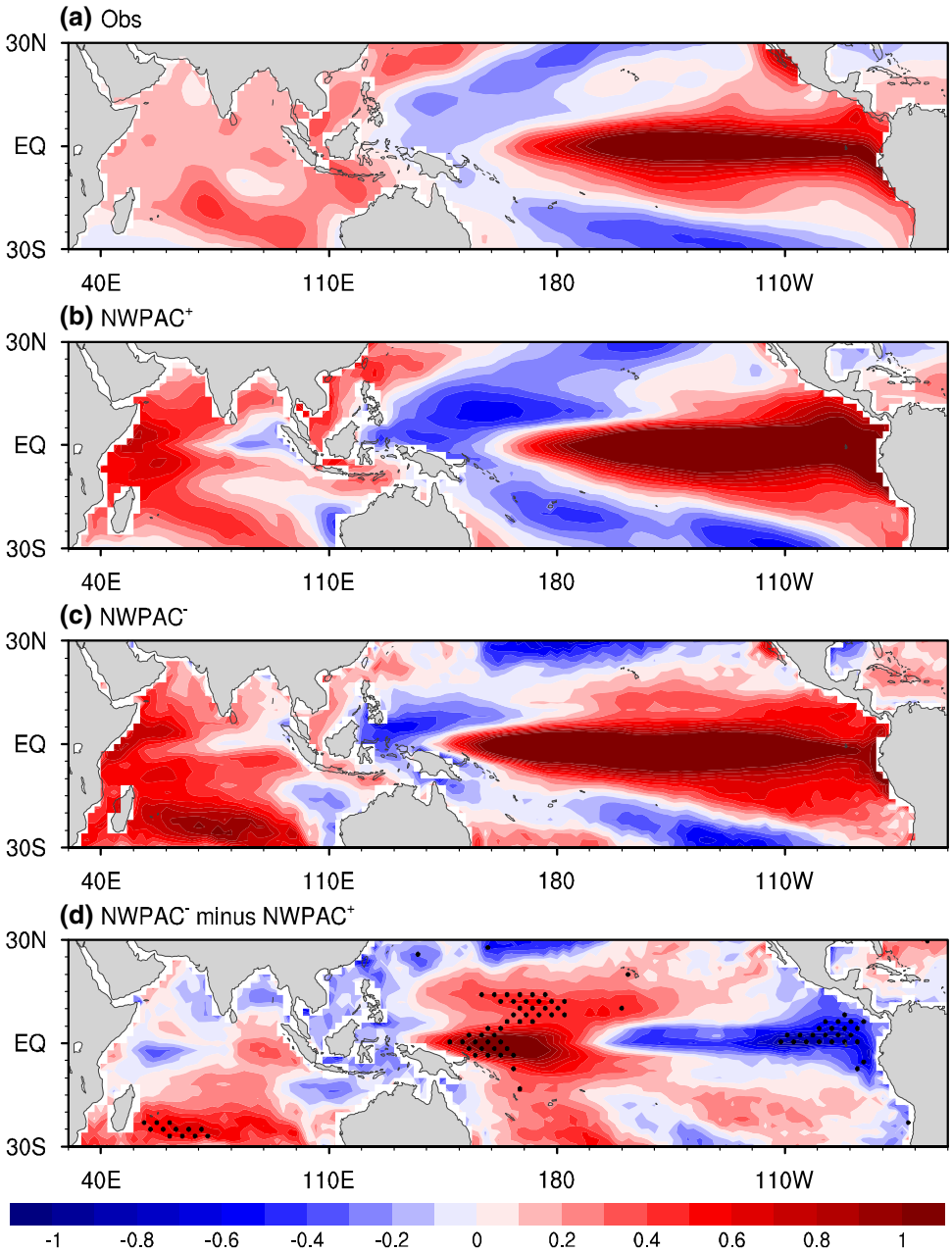

Fig. 6 Composited SST (°C) anomalies over the tropical Pacific and Indian Ocean during El Niño mature winters for **a** observations, **b** NWPAC$^+$ models, **c** NWPAC$^-$ models, and **d** the differences between NWPAC$^-$ and NWPAC$^+$ models. The stippling in **d** indicates the differences between NWPAC$^-$ and NWPAC$^+$ models exceeding the 0.05 significance level

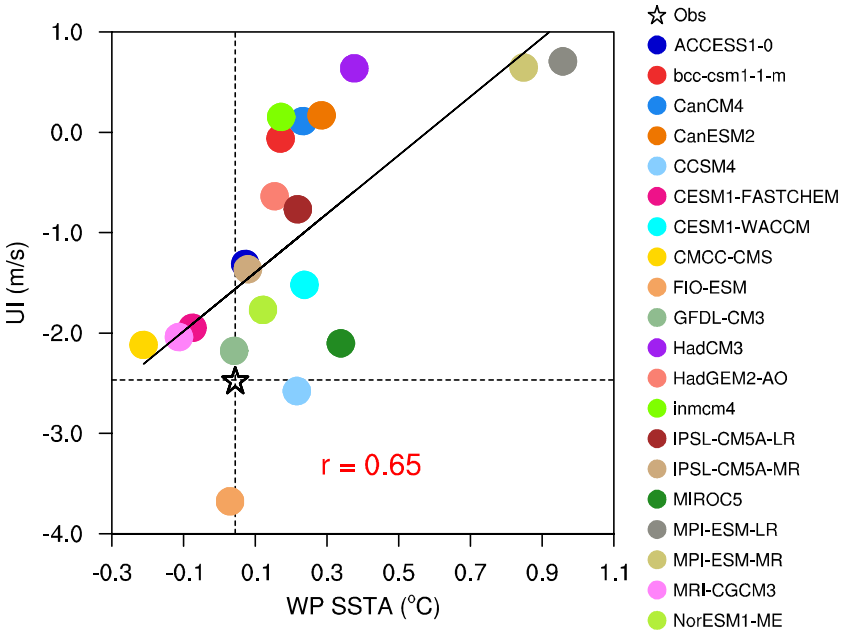

Fig. 7 Relationship between the SST anomalies averaged over the western Pacific (150°E–180°E, 6°S–6°N) and UI during post-El Niño summers among observations and 20 CMIP5 CGCMs. The inter-model correlation (r) is shown at the bottom

simulated El Niño SST anomalies over the western Pacific tend to have weaker tropical NWP anticyclonic anomalies during post-El Niño summers, with the inter-model correlations of 0.65. Statistically, the inter-model correlation coefficient exceeds the 0.01 significance level according to the Student's *t* test. This suggests that the excessive westward extension of simulated El Niño-related warm SST anomalies is important for the underestimation of tropical NWP circulation/rainfall anomalies during El Niño decaying summers in CMIP5 CGCMs.

The excessive westward extension of the simulated El Niño-related warm SST anomalies in the equatorial Pacific is associated with that of the simulated equatorial Pacific cold tongue that is a common bias in the mean state in CMIP5 CGCMs. Inter-model statistics supports this hypothesis. Indeed, models with a stronger equatorial Pacific cold tongue in the mean tend to display warmer SST anomaly biases in the equatorial western Pacific during post-El Niño summers, with an inter-model correlation of −0.61 exceeding the 0.01 significance level according to the Student's *t* test (Fig. 8a). To further highlight the effects of equatorial Pacific cold tongue bias on climate simulations, we choose four models (HadCM3, inmcm4, MPI-ESM-LR, and MPI-ESM-MR) of the lowest cold tongue SSTs as the cool cold tongue (cCT) models, and four models (CCSM4, CESM1-FASTCHEM, CMCC-CMS, and FIO-ESM) of the highest cold tongue SSTs as the warm cold tongue (wCT) models based on the mean SSTs over the equatorial Pacific cold tongue (160°E–90°W, 2°S–2°N) as shown in Fig. 8a. While wCT models well reproduce the observed pattern of El Niño SST anomalies, cCT models have an excessive westward extension of interannual SST warming along the equatorial Pacific and thus too warm SST anomalies in the equatorial western Pacific (Fig. 9). Meanwhile, the inter-model relationship between the equatorial Pacific cold tongue SSTs in the mean and Niño3.4 SST anomalies during El Niño mature winters is not statistically significant (r = 0.32; Fig. 8b). This implies that the equatorial Pacific cold tongue biases in CMIP5 CGCMs would not significantly affect the simulated amplitude of the El Niño-related SST anomalies but result in an excessive westward extension of interannual El Niño SST warming along the equatorial Pacific.

We now examine the relationship between the excessive equatorial Pacific cold tongue bias in the mean and underestimated El Niño-NWP summer teleconnections. Figure 10 shows the relationship of the equatorial Pacific cold tongue SSTs in the mean with the anomalous tropical NWP circulation and rainfall anomalies during post-El Niño summers among CMIP5 CGCMs. Models with a stronger equatorial Pacific cold tongue would exhibit weaker tropical NWP anticyclonic and negative rainfall anomalies, with the inter-model correlations of −0.74 and −0.71, respectively. Statistically, both the inter-model correlation coefficients exceed the 0.001 significance level according to the Student's *t* test. Thus, such underestimated El Niño teleconnections to the tropical NWP monsoon circulation and rainfall anomalies during post-El Niño summers in CMIP5 CGCMs can be traced back to the well-known excessive equatorial Pacific cold tongue error in the mean.

4.3 Physical process of error development

In Sect. 4.2, we have identified the statistical relationship between the excessive Pacific cold tongue bias and

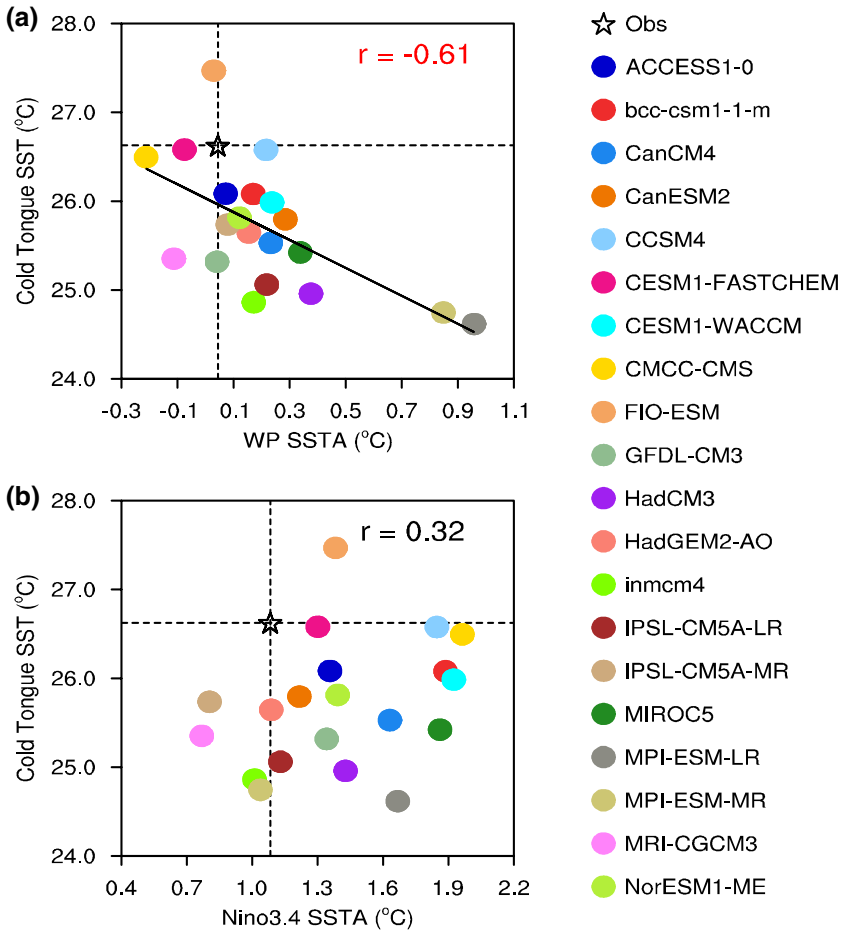

Fig. 8 Scatterplots of the mean SSTs over the equatorial Pacific cold tongue (160°E–90°W, 2°S–2°N) versus SST anomalies averaged over **a** the western Pacific during El Niño decaying summers and **b** the Niño3.4 region during El Niño mature winters among observations and 20 CMIP5 CGCMs. The inter-model correlation (r) is shown in each panel

underestimated tropical NWP pressure (anticyclonic) and rainfall anomalies during post-El Niño summers in CMIP5 CGCMs. However, it is still unclear how the Pacific cold tongue bias affects the simulations of El Niño-NWP summer teleconnections. Figure 11a–c show the composited differences in SST and 850-hPa streamfunction and rotational wind anomalies between cCT models and wCT models during El Niño mature winters, decaying springs, and decaying summers, respectively. Pronounced positive SST anomalies over the western Pacific indicate an excessive westward extension of El Niño SST warming along the equator. They can persist from El Niño mature winters to the following summers.

The western Pacific warming in cCT models during El Niño mature winters, decaying springs, and decaying summers enhances the local atmospheric convection and upper-level divergence, which is supported by the upper-level velocity potential and divergent wind (Fig. 12). The abnormal convective heating associated with the western Pacific upper-level divergence, in term of the Matsuno-Gill dynamics, induces low-level cyclonic circulation anomalies over the tropical NWP (Fig. 11), resulting in too weak an anticyclonic circulation response over the tropical NWP during post-El Niño summers in cCT models (Figs. 1, 2). This is essentially a Rossby wave circulation response to the enhanced convective heating. Such a Rossby wave response is also evident in tropospheric temperature. Owing to abnormal SST warming (Fig. 11c) and enhanced convective heating (Fig. 12c) in the western Pacific, tropospheric temperature is warmed over the tropical NWP in post-El Niño summers with physically consistent upper-level anticyclonic anomalies in cCT models (Fig. 13c). The resultant anomalous upper-level divergence over the tropical NWP promotes convective heating accompanied by anomalous low-level cyclonic circulation, leading to underestimated El Niño-induced tropical NWP summer anticyclonic anomalies in cCT models. All this highlights the importance of excessive westward extensions of simulated mean cold tongue and El Niño-related warm SST anomalies in the equatorial Pacific for the underestimated El Niño-NWP summer teleconnections in CMIP5 models.

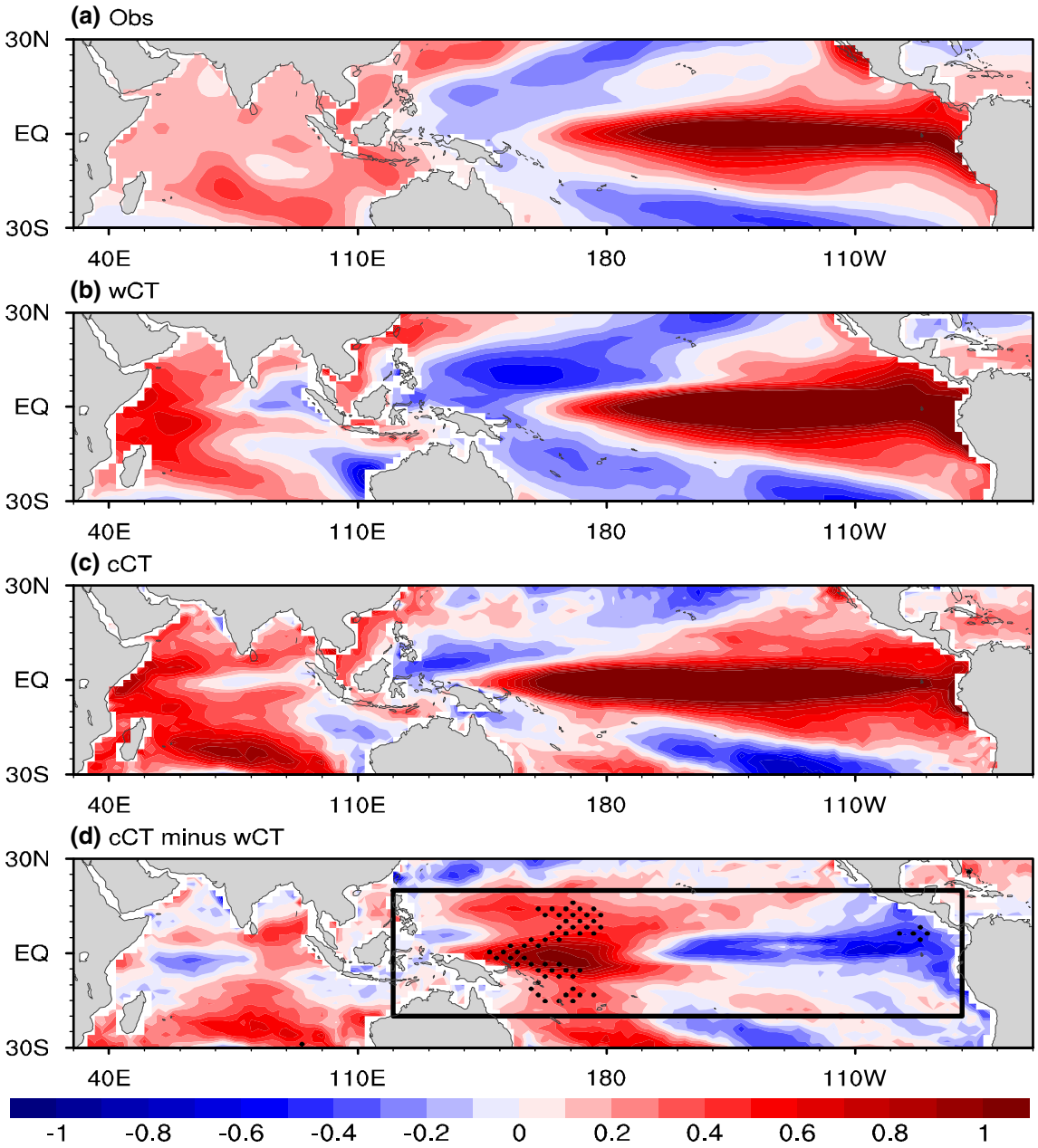

Fig. 9 Composited SST (°C) anomalies over the tropical Pacific and Indian Ocean during El Niño mature winters for **a** observations, **b** wCT models, and **c** cCT models, and **d** the differences between cCT and wCT models. The stippling in **d** indicates the differences between cCT and wCT models exceeding the 0.05 significance level. The black box in **d** shows the tropical Pacific region (120°E–80°W, 20°S–20°N) where the SST anomalies are used to force the sensitivity experiment (see Sect. 2.3 for details)

To further corroborate the effect of the bias pattern of El Niño SST anomalies related to the equatorial Pacific cold tongue bias, we perform an experiment by using the NCAR CAM4 as described in detail in Sect. 2.3. With the tropical Pacific bias pattern of El Niño SST anomalies (as shown in the black box of Fig. 9d) related to the equatorial Pacific cold tongue bias, the model reproduces the Gill-type Rossby circulation, precipitation, and tropospheric temperature responses (Fig. 14). The low-level cyclonic circulation biases over the tropical NWP associated with

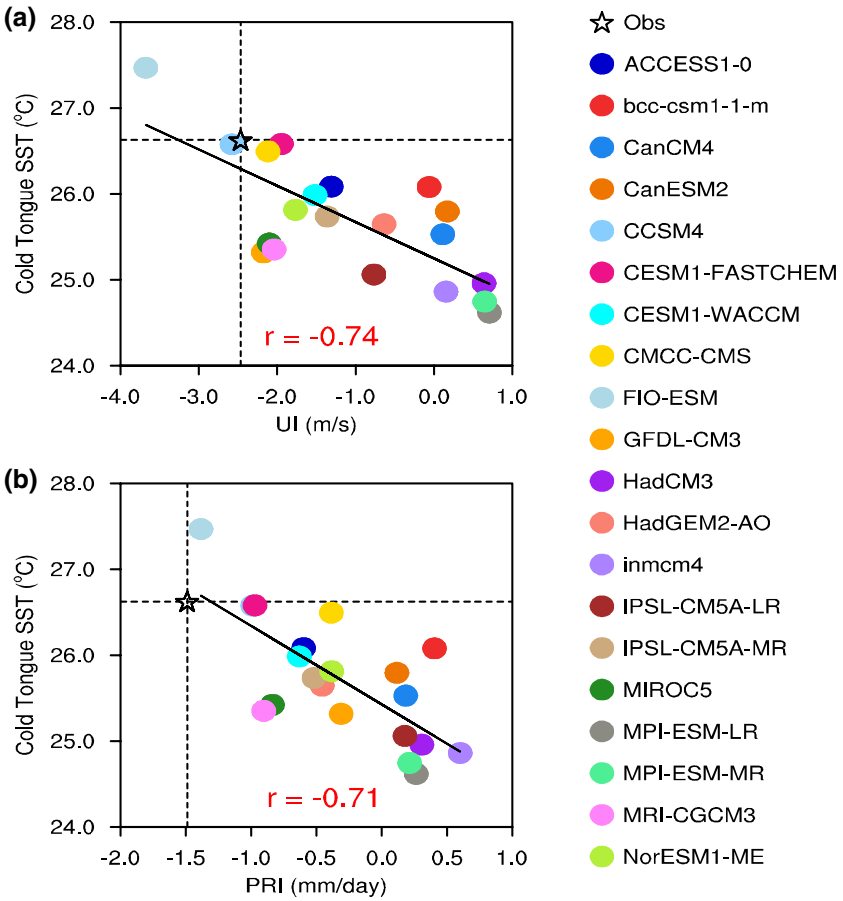

Fig. 10 Scatterplots of the mean SSTs over the equatorial Pacific cold tongue versus **a** UI and **b** PRI during El Niño decaying summers among observations and 20 CMIP5 CGCMs. The inter-model correlation (r) is shown in each panel

the equatorial Pacific cold tongue bias would weaken the tropical NWP anticyclone and rainfall anomalies during post-El Niño summers. As a result, CMIP5 CGCMs commonly have too weak El Niño-induced tropical NWP summer anticyclonic anomalies, consistent with the CMIP5 multi-model analysis. This confirms the role of the equatorial Pacific cold tongue bias in the underestimated El Niño-NWP summer monsoon teleconnections in CMIP5 CGCMs.

5 Summary and discussions

Observations show that El Niño events can induce coherent low-level anticyclonic circulation and negative rainfall anomalies over the tropical NWP, which persist from boreal winter to the following summer. The tropical NWP anomalies bridge the preceding winter eastern Pacific SST warming and the Asian summer monsoons, exerting important effects on summer climate anomalies over the Indo-western Pacific, East Asia, and South Asia. Unfortunately, CMIP5 CGCMs commonly underestimate such El Niño-NWP climate teleconnections with too weak tropical NWP pressure (anticyclonic) and rainfall anomalies during post-El Niño summers, potentially limiting the models' skill in predicting the Asian summer monsoons. The present analysis suggests that the underestimated El Niño teleconnections to the tropical NWP monsoon circulation and rainfall anomalies during post-El Niño summers in CMIP5 CGCMs can be traced back to the well-known excessive equatorial Pacific cold tongue error in the mean. Climate models with an excessive westward extension of Pacific cold tongue tend to displace westward the simulated pattern of El Niño warm SST anomalies along the equator. The resultant warm SST biases over the western Pacific during post-El Niño summers would enhance the local atmospheric convection/rainfall and upper-level divergence in CGCMs. The anomalous convective heating, in term of the Matsuno-Gill dynamics, induces low-level cyclonic circulation anomalies over the NWP, resulting in the commonly underestimated responses of anticyclonic circulation and rainfall during post-El Niño summers in CMIP5 CGCMs.

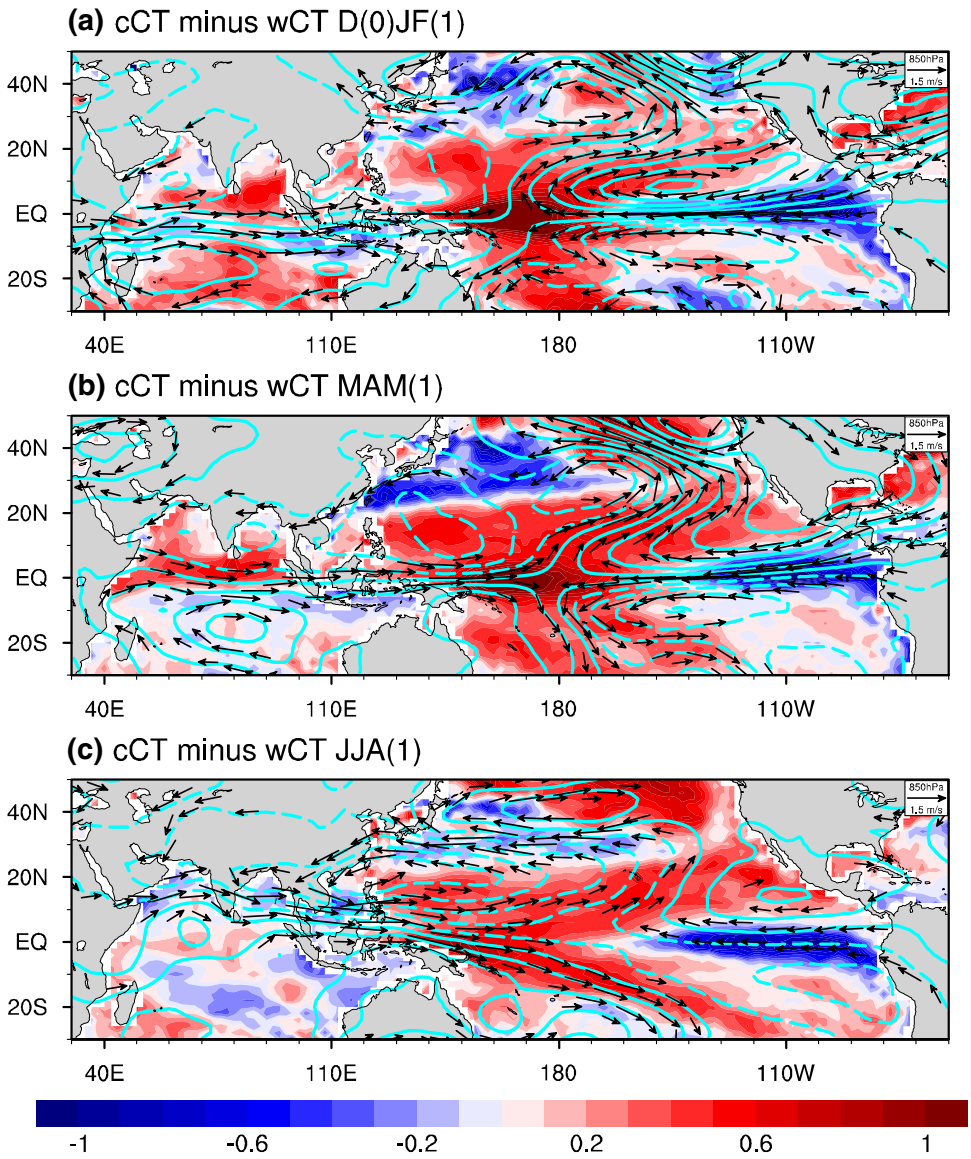

Fig. 11 cCT minus wCT composited differences of SST (color shaded, °C) and 850-hPa streamfunction (contour interval: $0.5 \times 10^6/s^1$) and rotational wind (vectors, m/s) anomalies during El Niño **a** mature winters, **b** decaying springs (March–May), and **c** decaying summers. Wind speeds smaller than 0.75 m/s have been masked out

The excessive westward extension of equatorial Pacific cold tongue has persisted in several generations of CGCMs over two decades (Li and Xie 2014; Li et al. 2015). The effects of this well-known error on regional climate simulation and prediction/projection beyond the cold tongue itself are previously overlooked to a large extent, for one important reason. The equatorial Pacific cold tongue error does not significantly affect the simulated El Niño amplitude, i.e., the interannual SST warming strength over the central and eastern equatorial Pacific (Figs. 8b, 9). The present study indicates that, however, the Pacific cold tongue bias can cause an excessive westward extension of the simulated El Niño SST warming pattern along the equatorial Pacific, leading to a commonly underestimated El Niño-NWP summer monsoon relationship via a Gill-type Rossby wave response in CMIP5 CGCMs. This would limit the models' skill of regional climate prediction. Here the predictability of anomalous tropical NWP anticyclone during boreal summers following El Niño is measured by the correlation between the Niño3.4 SST anomalies during El Niño mature winters and the UI during El Niño decaying summers. Indeed, models with an equatorial cold tongue bias tend to have a weaker predictability of anomalous tropical NWP anticyclone during boreal summers following El Niño, with the inter-model correlation of -0.67 exceeding the 0.001 significance level according to the Student's *t* test (Fig. 15).

In addition, our previous study (Li et al. 2016b) has also found that models with an excessive westward extension of

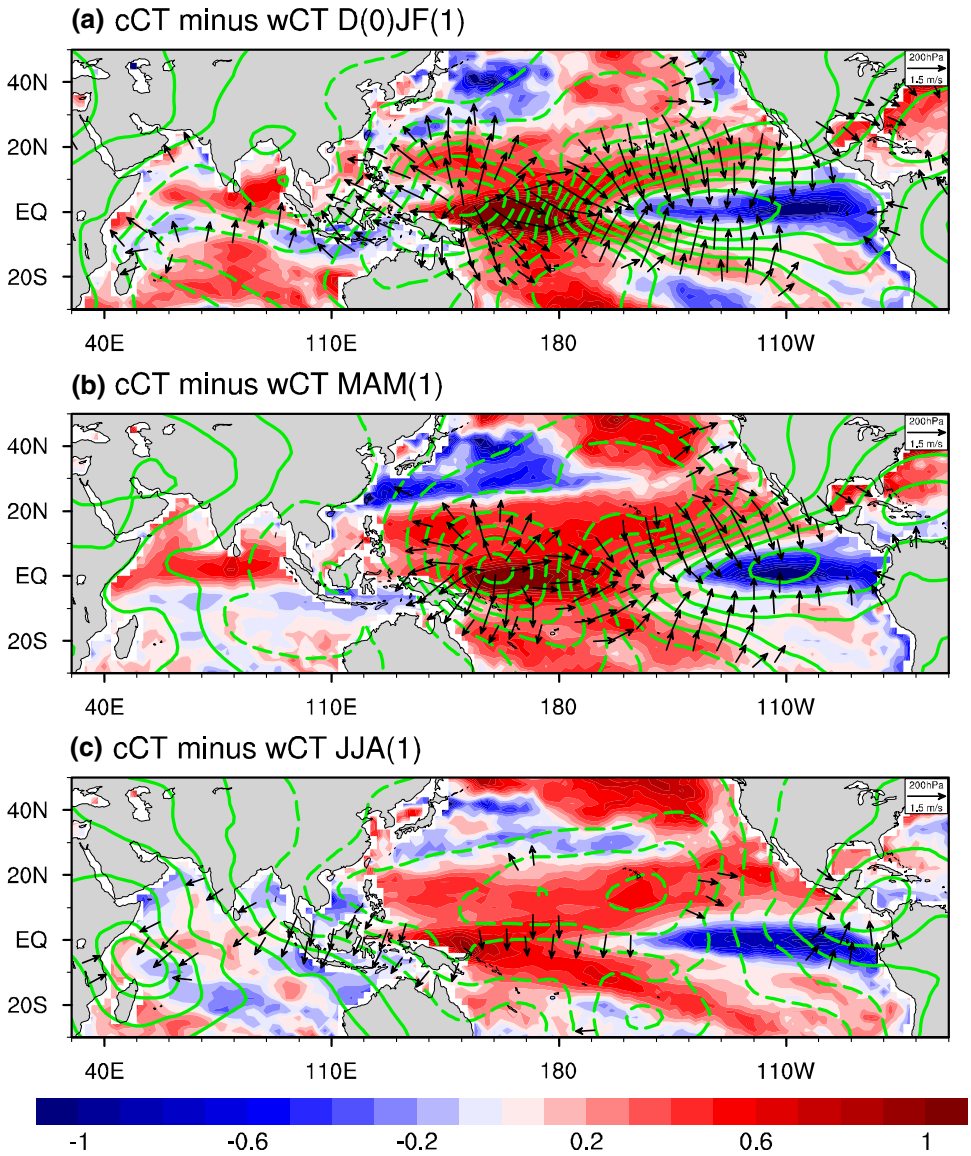

Fig. 12 Same as in Fig. 11, but for SST (color shaded, °C) and 200-hPa velocity potential (contour interval: 0.5×10^6 m^2/s) and divergent wind (vectors, m/s) anomalies

Pacific cold tongue tend to have insufficient mean precipitation/clouds over the equatorial western Pacific and thus a too weak local SST-convective feedback. This would result in an artificially amplified SST warming over the equatorial western Pacific under increased greenhouse gas scenario and then a La Niña-like offsetting error of tropical Pacific SST warming projection through Bjerknes feedback in CMIP5 CGCMs. These results highlight the importance of reducing equatorial Pacific cold tongue bias in CGCMs for improving climate simulation and prediction/projection for the tropical Pacific and Asian monsoons.

Multi-model statistics (Figs. 8, 9) suggest that the equatorial Pacific cold tongue biases in CMIP5 CGCMs do not significantly affect the simulated El Niño amplitude but result in an excessive westward extension of interannual El Niño SST warming along the equatorial Pacific. We assume that an excessive equatorial cold tongue in CGCMs may enhance the mean SST gradient over the equatorial western Pacific. During an El Niño event, the westerly winds burst on the equator and drive an anomalous eastward current. With a stronger mean west–east gradient of SST $\left(-\frac{\partial T}{\partial x}\right)$, the anomalous eastward flow (u') would probably bring about a larger anomalous warm advection $\left(-u'\frac{\partial T}{\partial x}\right)$, especially near

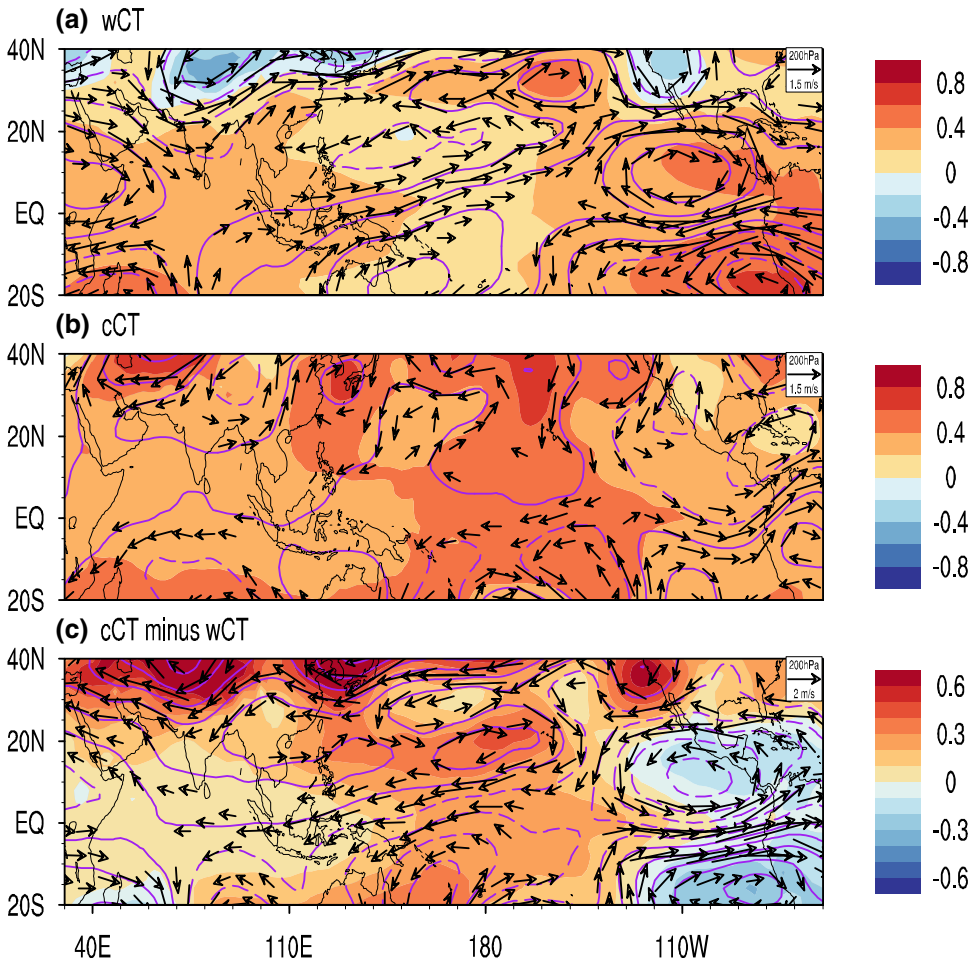

Fig. 13 Composited anomalies of 850–200 hPa mean tropospheric temperature (color shaded, °C) and 200-hPa streamfunction (contour interval: $1 \times 10^6/s^1$) and rotational winds (vectors, m/s) during El Niño decaying summers for **a** wCT models, **b** cCT models, and **c** cCT models minus wCT models. Wind speeds smaller than 0.75 m/s in **a** and **b** and 1 m/s in **c** have been masked out, respectively

the equatorial SST frontal zone, and thus result in warmer SST anomalies over the equatorial western Pacific, i.e., the excessive westward extension of simulated warm El Niño SST anomalies along the equatorial Pacific. This issue will be explored and discussed thoroughly in the future work. It is still unclear why the simulated El Niño amplitude cannot be significantly affected by the excessive cold tongue bias. We suppose that, on the one hand, an excessive cold tongue is accompanied by the surface easterly wind bias with too shallow a thermocline over the equatorial eastern Pacific in oceanic models (Li and Xie 2012, 2014; Zheng et al. 2012). This would enhance the SST-thermocline feedback in the eastern equatorial Pacific and thus facilitate the development of El Niño SST anomalies. On the other hand, a too cool cold tongue is linked to the insufficient precipitation/clouds in the equatorial Pacific in atmospheric models (Li et al. 2015, 2016b). This would weaken the response of equatorial Pacific convection/precipitation and in turn the zonal wind feedback to warm SST anomalies, suppressing the El Niño development. The two effects might counteract each other. As a result, the relationship between the simulated excessive cold tongue bias and El Niño amplitude is not statistically significant (Fig. 8b). This issue would be worthy of further investigation in the future work.

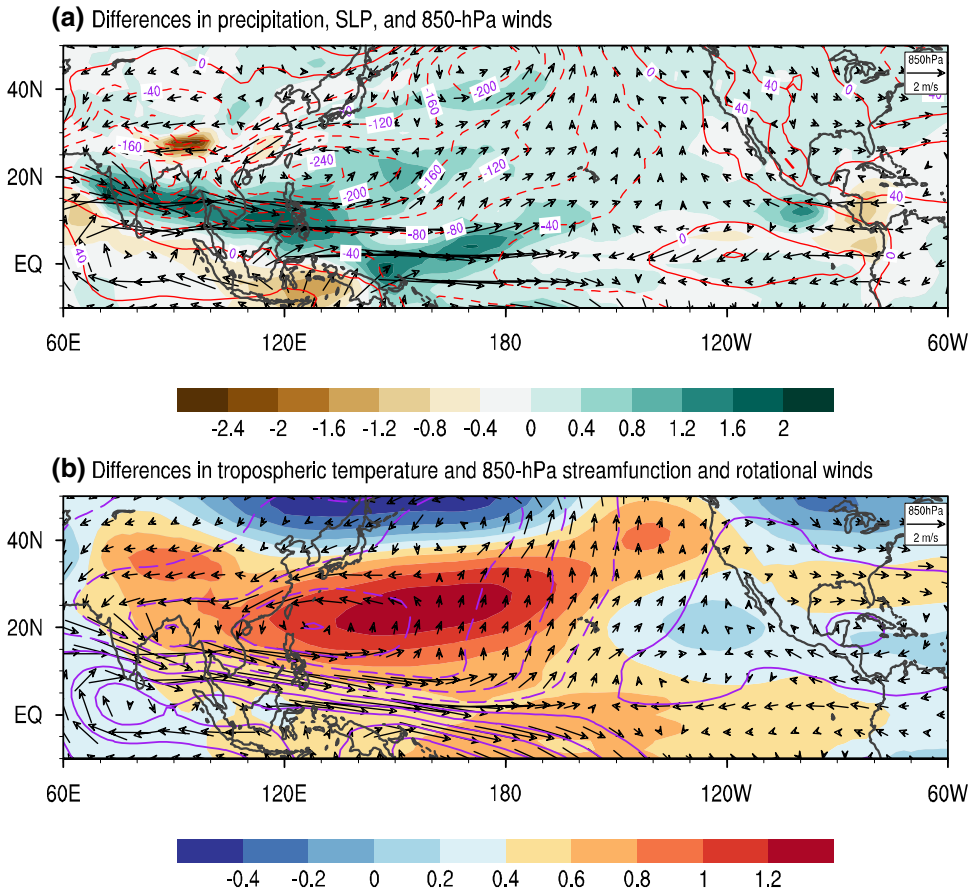

Fig. 14 Exp_SE minus Exp_CNTL differences in **a** precipitation (color shaded, mm/day), SLP (contours, Pa), and 850-hPa winds (vectors, m/s) and **b** 850–200 hPa mean tropospheric temperature (color shaded, °C) and 850-hPa streamfunction (contour interval: $0.5\times10^6/s^1$) and rotational winds (vectors, m/s) for El Niño decaying summers. Here the tropical Pacific bias pattern of El Niño SST anomalies used to force the sensitivity experiment is that included in the black box of Fig. 9d

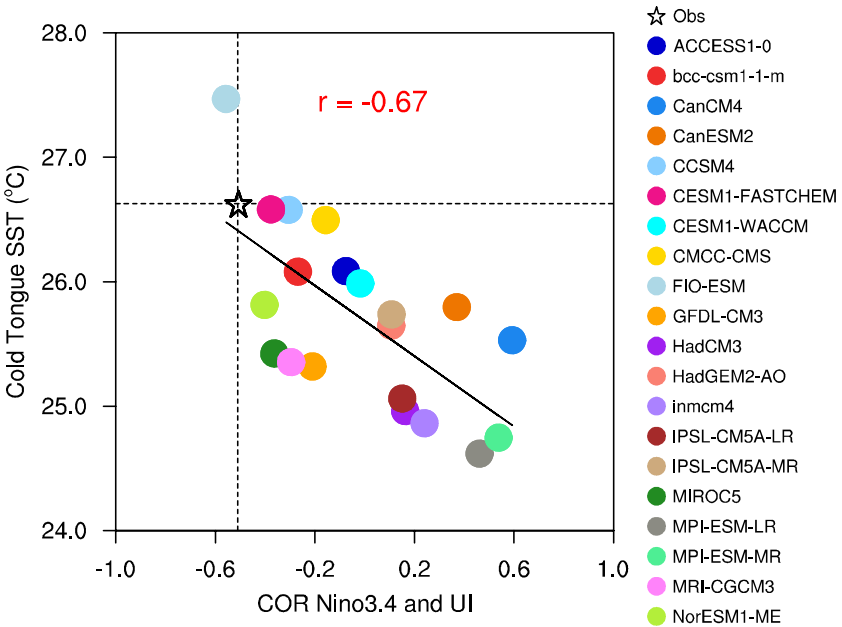

Fig. 15 Relationship between the mean SSTs over the equatorial Pacific cold tongue and the predictability of anomalous tropical NWP anticyclone during boreal summers following El Niño among observations and 20 CMIP5 CGCMs. Here the predictability of anomalous tropical NWP anticyclone during boreal summers following El Niño is characterized by the correlation coefficient between the Niño3.4 SST anomalies during El Niño mature winters and UI during El Niño decaying summers. The inter-model correlation (r) is shown on the top

Acknowledgements This work was supported by the Fundamental Research Funds for the Central Universities (2018B03114), the Natural Science Foundation of China (41831175, 41690123, 41690120, and 41406026), the Research Fund Program of Guangdong Province Key Laboratory for Climate Change and Natural Disaster Studies (2017CCND003), the Guangdong Natural Science Funds for Distinguished Young Scholar (2015A030306008), the Youth Innovation Promotion Association CAS, and the Pearl River S&T Nova Program of Guangzhou (201506010094). We wish to thank the climate modeling groups (Table 1) for producing and making available their model outputs, the WCRP's Working Group on Coupled Modeling (WGCM) for organizing the CMIP5 analysis activity, the Program for Climate Model Diagnostics and Intercomparison (PCMDI) for collecting and archiving the CMIP5 multi-model data, and the Office of Science, US Departmentof Energy for supporting these datasets in partnership with the Global Organization for Earth System Science Portals.

References

Alexander MA, Blade´ I, Newman M, Lanzante JR, Lau NC, Scott JD (2002) The atmospheric bridge: the influence of ENSO teleconnections on air–sea interaction over the global oceans. J Clim 15:2205–2231

Chang CP, Zhang YS, Li T (2000) Interannual and interdecadal variations of the East Asian summer monsoon and tropical Pacific SSTs. Part I: Roles of the subtropical ridge. J Clim 13:4310–4325

Chowdary JS, Xie S-P, Luo J-J, Hafner J, Behera S, Masumoto Y, Yamagata T (2011) Predictability of Northwest Pacific climate during summer and the role of the tropical Indian Ocean. Clim Dyn 36:607–621

Chowdary JS, Gnanaseelan C, Chakravorty S (2013) Impact of northwest Pacific anticyclone on the Indian summer monsoon region. Theor Appl Climatol 113:329–336

De Szoeke SP, Xie S-P (2008) The tropical eastern Pacific seasonal cycle: Assessment of errors and mechanisms in IPCC AR4 coupled ocean–atmosphere general circulation models. J Clim 21:2573–2590

Dee DP et al (2011) The ERA-interim reanalysis: configuration and performance of the data assimilation system. Q J R Meteor Soc 137:553–597

Du Y, Xie S-P, Huang G, Hu K (2009) Role of air-sea interaction in the long persistence of El Niño-induced North Indian Ocean warming. J Clim 22:2023–2038

Du Y, Yang L, Xie S-P (2011) Tropical Indian Ocean influence on Northwest Pacific tropical cyclones in summer following strong El Niño. J Clim 24:315–322

Gent PR et al (2011) The community climate system model version 4. J Clim 24:4973–4991

Gill AE (1980) Some simple solutions for heat-induced tropical circulation. Q J R Meteor Soc 106:447–462

Hu K, Huang G, Zheng X-T, Xie S-P, Qu X, Du Y, Liu L (2014) Interdecadal variations in ENSO influences on Northwest Pacific-East Asian early summertime climate simulated in CMIP5 Models. J Clim 27:5982–5998

Huang R, Sun F (1992) Impacts of the tropical western Pacific on the East Asian summer monsoon. J Meteor Soc Jpn 70:243–256

Huang R, Wu Y (1989) The influence of ENSO on the summer climate change in China and its mechanism. Adv Atmos Sci 6:21–32

Hurrell J, Hack J, Shea D, Caron J, Rosinski J (2008) A new sea surface temperature and sea ice boundary data set for the Community Atmosphere Model. J Clim 21:5145–5153

Jiang W, Huang G, Hu K, Wu R, Gong H, Chen X, Tao W (2017) Diverse relationship between ENSO and Northwest Pacific summer climate among CMIP5 models: dependence on the ENSO decay pace. J Clim 30:109–127

Kalnay E et al (1996) The NCEP/NCAR 40-year reanalysis project. Bull Am Meteorol Soc 77:437–471

Klein SA, Soden BJ, Lau N-C (1999) Remote sea surface temperature variations during ENSO: evidence for a tropical atmospheric bridge. J Clim 12:917–932

Kosaka Y, Xie S-P, Lau N-C, Vecchi GA (2013) Origin of seasonal predictability for summer climate over the Northwestern Pacific. Proc Natl Acad Sci USA 110:7574–7579

Latif M et al (2001) ENSIP: the El Niño simulation intercomparison project. Clim Dyn 18:255–276

Li G, Xie S-P (2012) Origins of tropical-wide SST biases in CMIP multi-model ensembles. Geophys Res Lett 39:L22703. https://doi.org/10.1029/2012GL053777

Li G, Xie S-P (2014) Tropical biases in CMIP5 multimodel ensemble: the excessive equatorial Pacific cold tongue and double ITCZ problems. J Clim 27:1765–1780

Li G, Du Y, Xu H, Ren B (2015) An intermodel approach to identify the source of excessive equatorial Pacific cold tongue in CMIP5 models and uncertainty in observational datasets. J Clim 28:7630–7640

Li G, Xie S-P, Du Y (2016a) A robust but spurious pattern of climate change in model projections over the tropical Indian Ocean. J Clim 29:5589–5608

Li G, Xie S-P, Du Y, Luo Y (2016b) Effects of excessive equatorial cold tongue bias on the projections of tropical Pacific climate change. Part I: the warming pattern in CMIP5 multi-model ensemble. Clim Dyn 47:3817–3831

Li G, Xie S-P, He C, Chen Z (2017) Western Pacific emergent constraint lowers projected increase in Indian summer monsoon rainfall. Nat Clim Change 7:708–712

Lin J-L (2007) The double-ITCZ problem in IPCC AR4 coupled GCMs: ocean–atmosphere feedback analysis. J Clim 20:4497–4525

Liu F, Lu J, Garuba O, Leung LR, Luo Y, Wan X (2018) Sensitivity of surface temperature to oceanic forcing via q-flux Green's function experiments. Part I: Linear response function. J Clim 31:3625–3641

Lu R, Lu S (2015) Asymmetric relationship between Indian Ocean SST and the Western North Pacific Summer Monsoon. J Clim 28:1383–1395

Matsuno T (1966) Quasi-geostrophic motions in the equatorial area. J Meteor Soc Jpn 44:25–43

Mechoso CR et al (1995) The seasonal cycle over the tropical Pacific in coupled ocean–atmosphere general circulation models. Mon Weather Rev 123:2825–2838

Mishra V, Smoliak BV, Lettenmaier DP, Wallace JM (2012) A prominent pattern of year-to-year variability in Indian Summer Monsoon rainfall. Proc Natl Acad Sci USA 109:7213–7217

Nitta T (1986) Long-term variations of cloud amount in the western Pacific region. J Meteor Soc Jpn 64:373–390

Nitta T (1987) Convective activities in the tropical western Pacific and their impacts on the Northern Hemisphere summer circulation. J Meteor Soc Jpn 65:165–171

Smith TM, Reynolds RW, Peterson TC, Lawrimore J (2008) Improvements to NOAA's historical merged land–ocean temp analysis (1880–2006). J Clim 21:2283–2296

Stuecker MF, Timmermann A, Jin F-F, McGregor S, Ren H-L (2013) A combination mode of the annual cycle and the El Niño/Southern Oscillation. Nat Geosci 6:540–544

Stuecker MF, Jin F-F, Timmermann A, McGregor S (2015) Combination mode dynamics of the anomalous Northwest Pacific anticyclone. J Clim 28:1093–1111

Taylor KE, Ronald JS, Meehl GA (2012) An overview of CMIP5 and the experiment design. Bull Am Meteorol Soc 93:485–498

Trenberth KE, Branstator GW, Karoly D, Kumar A, Lau N-C, Ropelewski C (1998) Progress during TOGA in understanding and modeling global teleconnections associated with tropical sea surface temperatures. J Geophys Res 103:14291–14324

Wang C, Weisberg RH, Virmani JI (1999) Western Pacific interannual variability associated with the El Niño-Southern Oscillation. J Geophys Res 104:5131–5149

Wang B, Wu R, Fu X (2000) Pacific-East Asian teleconnection: how does ENSO affect East Asian climate? J Clim 13:1517–1536

Wang B, Wu RG, Lau K-M (2001) Interannual variability of the Asian summer monsoon: contrasts between the Indian and the western North Pacific-East Asian monsoons. J Clim 14:4073–4090

Wang C, Wang W, Wang D, Wang Q (2006) Interannual variability of the South China Sea associated with El Niño. J Geophys Res 111:C03023. https://doi.org/10.1029/2005JC003333

Webster PJ, Yang S (1992) Monsoon and ENSO: selectively interactive systems. Q J R Meteor Soc 118:877–926

Wu R, Hu ZZ, Kirtman BP (2003) Evolution of ENSO-related rainfall anomalies in East Asia. J Clim 16:3742–3758

Xie P, Arkin PA (1997) Global precipitation: a 17-year monthly analysis based on gauge observations, satellite estimates, and numerical model outputs. Bull Am Meteorol Soc 78:2539–2558

Xie S-P, Hu K, Hafner J, Tokinaga H, Du Y, Huang G, Sampe T (2009) Indian Ocean capacitor effect on Indo-western Pacific climate during the summer following El Niño. J Clim 22:730–747

Xie S-P, Kosaka Y, Du Y, Hu KM, Chowdary J, Huang G (2016) Indo-western Pacific ocean capacitor and coherent climate anomalies in post-ENSO summer: a review. Adv Atmos Sci 33:411–432

Yang JL, Liu QY, Xie S-P, Liu ZY, Wu LX (2007) Impact of the Indian Ocean SST basin mode on the Asian summer monsoon. Geophys Res Lett 34:L02708. https://doi.org/10.01029/02006GL028571

Yoo SH, Yang S, Ho CH (2006) Variability of the Indian Ocean sea surface temperature and its impacts on Asian–Australian monsoon climate. J Geophys Res 111:D03108. https://doi.org/10.1029/2005JD006001

Yu J-Y, Mechoso CR (1999) Links between annual variations of Peruvian stratocumulus clouds and of SST in the eastern equatorial Pacific. J Clim 12:3305–3318

Zhang R, Sumi A, Kimoto M (1996) Impact of El Niño on the East Asian monsoon: a diagnostic study of the'86/87 and'91/92 events. J Meteor Soc Jpn 74:49–62

Zheng Y, Lin J-L, Shinoda T (2012) The equatorial Pacific cold tongue simulated by IPCC AR4 coupled GCMs: upper ocean heat budget and feedback analysis. J Geophys Res 117:C05024. https://doi.org/10.1029/2011JC007746